# Supplementary information

## Heteropoly Acid-Mediated Electrochemical Efficiency Removal of Oxygen

**Authors**

Peilin Sun [a†], Peng Wang [a†], Zhaoxi Chen [a†], An Pei [a], Qiqi Wu [a], Gaige Zhang [a], Sijia Ji [a], Daoru Liu [a], Haohang Qin [a], and Guangxu Chen *[a]

**Affiliations**

a. School of Environment and Energy, National Engineering Laboratory for VOCs Pollution Control Technology and Equipment, Guangdong Provincial Key Laboratory of Atmospheric Environment and Pollution Control, South China University of Technology, Guangzhou 510006, China

## Experimental Procedures

### Chemicals

Silicotungstic acid hydrate ($H_4[SiW_{12}O_{40}]\cdot xH_2O$, AR), phosphoric acid solution (60 wt%), sodium hydroxide (NaOH, 97%), and copper sulfate ($CuSO_4\cdot 5H_2O$, 99%) were purchased from Aladdin; potassium sodium tartrate ($NaKC_4H_4O_6\cdot 4H_2O$, 99%) and bovine serum albumin (BSA, 96%) were obtained from Maclean's. Nafion 117 cation exchange membrane (CEM), anion exchange membrane (AEM) (FAA-3-PK-130), carbon paper (GDL-3250) (Fuel Cell Store), 20% Pt/C catalyst (Johnson Matthey), carbon felts, and iridium oxide-coated titanium mesh were sourced from Alibaba Taobao Store. Ultrapure water (18.2 MΩ·cm) was used for all electrolyte preparations. Milk (Yili Group) and perishables (tofu, celery, bananas, cucumbers) were procured from a local retail supplier.

### Preparation of gas diffusion electrode

Typically, 10 mg of Pt/C catalyst is mixed with 50 μL of 5 wt% Nafion solution and 1 mL of a 1:1 (v/v) ethanol/water solvent mixture. The solution is sonicated for at least 60 minutes at room temperature. The well-dispersed ink is then sprayed onto a GDL-3250 (2 × 2 $cm^2$) using an air compressor to pump the gun (HD-180) at a constant pressure, and the sample is then dried. This process was confirmed by weighing the GDE before and after spraying, resulting in a loading of approximately 1.0 $mg/cm^2$. Finally, 10 mg of carbon black and 500 μL of 60% polytetrafluoroethylene emulsion are added to 20 mL of ethanol, and the mixture is sonicated for 1 hour. Then, 100 μL of the resulting ink is sprayed onto the catalyst layer surface and dried.

### ORR in a flow cell

The gas-tight flow cell system included one gas chamber and two liquid chambers, with peristaltic pumping of a 1 M KOH aqueous solution serving as the anode and cathode electrolytes at a rate of 20 mL/min. The airflow rate was maintained at 20 mL/min using a peristaltic pump. Iridium oxide titanium mesh was used for OER. An anion exchange membrane separated the cathode and anode solutions. Electrolysis was conducted using a BioLogic VMP3 electrochemical workstation with two electrodes.

### Hydrolysis of biuret reagents

Dissolve 1.5 g of copper sulfate ($CuSO_4\cdot 5H_2O$) and 6.0 g of potassium sodium tartrate ($NaKC_4H_4O_6\cdot 4H_2O$) in 500 mL of water. Add 300 mL of 10% NaOH (w/v) solution, mix thoroughly, and then dilute to 1 L.

### Construction and operation of the EMAORS

The EMAORS is a two-electrode flow-through electrolytic cell (active area: 2 × 2 $cm^2$) separated by a layer of Nafion 117 CEM (untreated and used as-is), with a 2 × 2 $cm^2$ titanium mesh coated with iridium oxide acting as the anode ($IrO_2$ loading: 1 $mg/cm^2$) and a carbon felt (untreated) acting as the cathode. ERSS tests were performed on a BioLogic VMP3 workstation. All experiments were performed at room temperature (25°C) and at ambient pressure. The cathode electrolyte, electrolytic

cell, gas dryer (which removes entrained water vapor from the silicotungstic acid solution), and the separation unit formed a closed system. Oxygen content was monitored in real time with an oxygen analyzer (JC-D2200), and the food was then placed in the separation unit. 50 mM of the silicotungstic acid electrolyte, 1.19 wt% of the phosphoric acid solution, and the air in the closed system were pumped in at a flow rate of 20 mL/min, and circulated between the cathode and the anode, respectively. The air in the closed system was pumped at a flow rate of 20 mL/min and circulated between the cathode and anode, respectively.

**Electrolyte preparation**

2 mL of concentrated $H_3PO_4$ solution was mixed with 100 mL of water to prepare a 1.19 wt% % phosphoric acid solution as the anode electrolyte. For the cathode electrolyte, 4.32 g (30 mL system) or 71.95 g (500 mL system) of silicotungstic acid hydrate ($H_4[SiW_{12}O_{40}]\cdot xH_2O$) was dissolved in an equivalent 1.19 wt% $H_3PO_4$ solution, yielding 50 mM silicotungstic acid concentrations through magnetic stirring.

**PGCS operation**

The PGCS replicated EMAORS hydrodynamic conditions by circulating air through identical food-containing separation units at a 20 mL/min flow rate using equivalent peristaltic pumps, while bypassing the electrochemical oxygen removal module.

**Determination of protein content**

1 mL of each standard solution with concentrations of 0, 2, 4, 6, and 8 mg/L BSA was prepared. To each tube, 4 mL of biuret reagent was added, and the mixtures were then thoroughly mixed and allowed to stand at room temperature for 20 minutes. The absorbance was measured at 540 nm using a spectrophotometer (UV-1500PC), and a standard curve was plotted with protein concentration on the x-axis and absorbance on the y-axis. Take 1 mL of the 10-fold diluted milk sample, add 4 mL of biuret reagent, mix thoroughly, and let it stand at room temperature for 20 minutes. Measure the absorbance at 540 nm with a spectrophotometer and determine the protein concentration from the standard curve.

**Techno-economic analysis**

In terms of long-term operational material inputs, the EMAORS system primarily relies on two basic resources: electricity and water. In contrast, the conventional ORR system requires additional consumption of the chemical reagent KOH. To quantitatively compare the costs of the two systems, this study conducted calculations based on an established economic analysis framework. The assumptions include a daily oxygen removal capacity of 100 L ($V_{daily}$), 350 operating days per year ($t_{annual}$), an industrial electricity price of 0.02 USD/kWh ($p_{elec}$), a purified water cost of 0.7 USD/t ($p_{H2O}$), and a KOH price of 820 USD/t ($p_{KOH}$).[1, 2]

The electricity cost is calculated as follows:

$$C_{elec,EMAORS} = E_{EMAORS} * V_{daily} * t_{annual} * p_{elec} = 0.013 * 100 * 350 * 0.02 = 9.1\ USD$$

$$C_{elec,ORR} = E_{ORR} * V_{daily} * t_{annual} * p_{elec} = 0.016 * 100 * 350 * 0.02 = 11.2\ USD$$

Regarding water consumption, since both systems exhibit oxygen evolution reaction (OER) at the anodes and follow a four-electron transfer pathway at the cathodes, their theoretical water consumption is identical. Based on the stoichiometric relationship of the reactions, the mass of water required is:

$$C_{H_2O} = \frac{V_{O_2}}{V_m} * n_{H_2O} * M_{H_2O} * t_{annual} * p_{water} = \frac{100}{22.4} * 2 * 18 * 10^{-6} * 350 * 0.7 \approx 0.04\ USD$$

Standard molar volume ($V_m$)=22.4 L/mol, molar mass of water ($M_{H2O}$)=18 g/mol, water consumption per mole of $O_2$ ($n_{H2O}$)=2 mol。

Traditional ORR systems also incur ongoing costs for KOH consumption. Their electrolyte readily reacts with acidic gases like $CO_2$ in the air to form $K_2CO_3$, which not only causes the alkaline solution to become ineffective but may also lead to flow channel blockages due to carbonate crystallization. To maintain performance, taking the example of replacing 1 L of 1 M KOH solution every two weeks, the annual KOH consumption by mass is:

$$m_{KOH} = C_{KOH,sol} * V_{sol} * M_{KOH} * N_{change} * p_{KOH} = 1 * 1 * 56 * 24 * 10^{-6} * 820 \approx 1.07\ USD$$

The corresponding water cost is:

$$C_{H_2O,ORR} = V_{sol} * N_{change} * p_{water} = 1 * 24 * 10^{-3} * 0.7 \approx 0.02\ USD$$

The concentration of the KOH solution ($C_{KOH,sol}$)=1 M, the volume replaced each time ($V_{sol}$)=1, the molar mass of KOH ($M_{KOH}$)=56 g/mol, the number of replacements per year ($N_{change}$)=24.

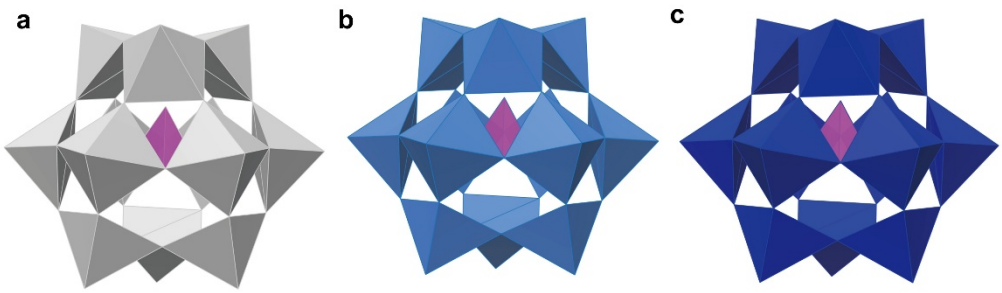


***Figure S1.*** The polyhedral framework model of silicotungstic acid. (a) $H_4[SiW_{12}O_{40}]$. (b) $H_5[SiW_{12}O_{40}]$. (c) $H_6[SiW_{12}O_{40}]$.

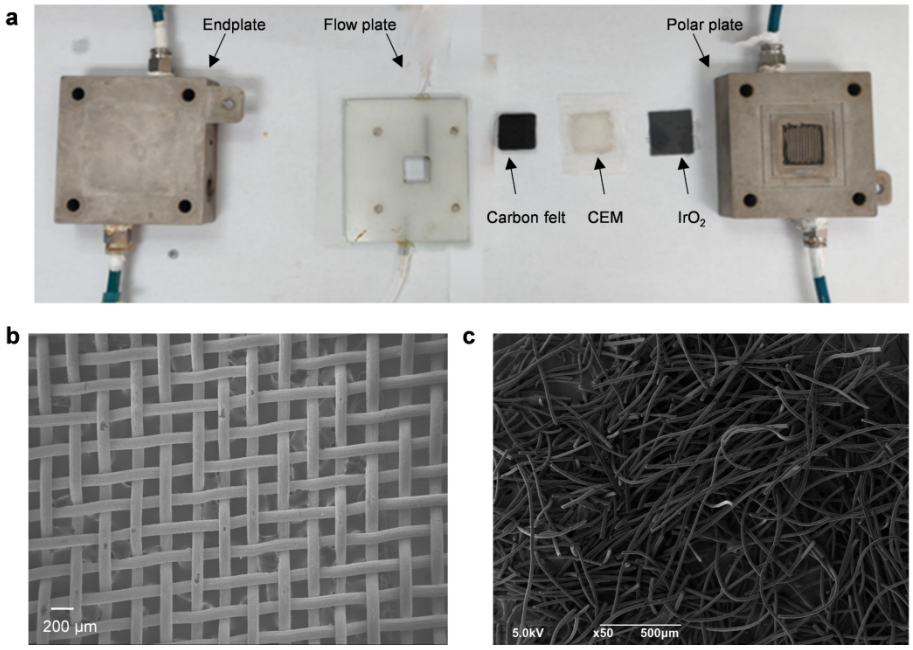


***Figure S2.*** (a) Photograph and layout of the disassembled electrolytic cell components. Scanning electron microscopy (SEM) image of the iridium oxide-coated titanium mesh anode (b) and the carbon felt cathode (c).

*Note:* Characterization was performed using scanning electron microscopy (SEM; ZEISS, Merlin).

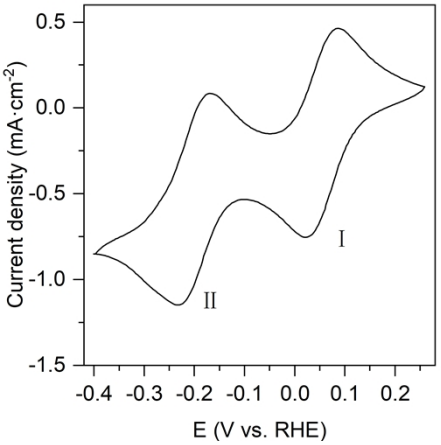


***Figure S3.*** CV curve of silicotungstic acid solution (Assignment of reduction waves: wave I ($H_4 \rightarrow H_5$); wave II ($H_5 \rightarrow H_6$)).

*Note:* Cyclic voltammogram of 0.05 M $H_4[SiW_{12}O_{40}]$ in aqueous solution (pH 1) under argon atmosphere at room temperature. A glassy carbon working electrode (area = 0.19625 $cm^2$), a Pt-mesh counter electrode, and an Ag/AgCl reference electrode were used. Scan rate: 0.1 V/s.

$$E_{RHE} = E_{Ag/AgCl} + 0.0592 \times pH + 0.197$$

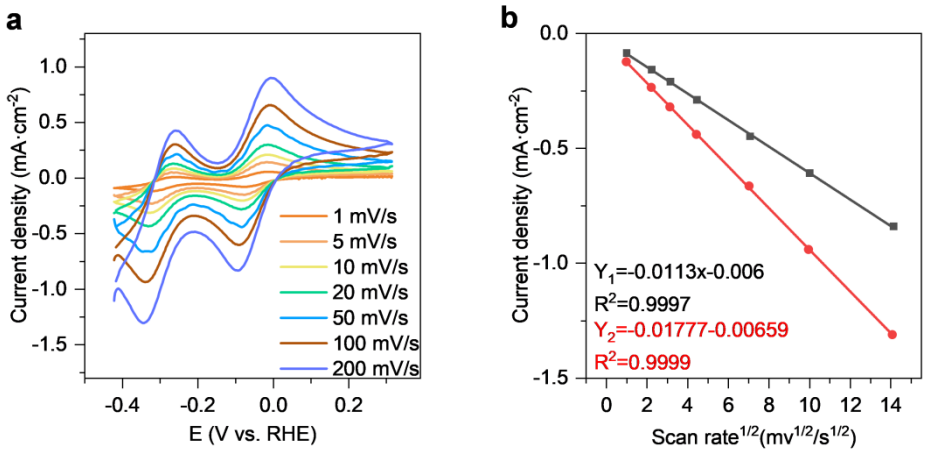


***Figure S4.*** (a) CV curves of silicotungstic acid solution at different scan rates (under Ar and at room temperature). (b) Linear fitting of scan rate versus cathodic peak current.

*Note:* $Y_1$ and $Y_2$ correspond to the linear relationships between the first and second cathodic peak currents and the square root of the scan rate, respectively.[3]

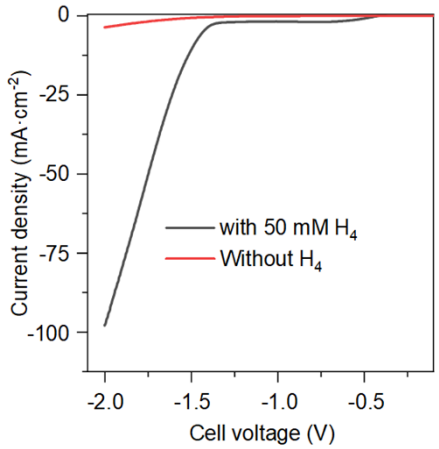


***Figure S5.*** LSV profiles of $H_3PO_4$ solution with and without 50 mM $H_4$ in an Ar atmosphere.

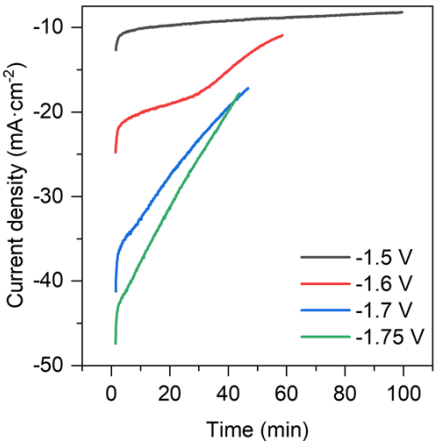


***Figure S6.*** Current curves of silicotungstic acid solution at different potentials.

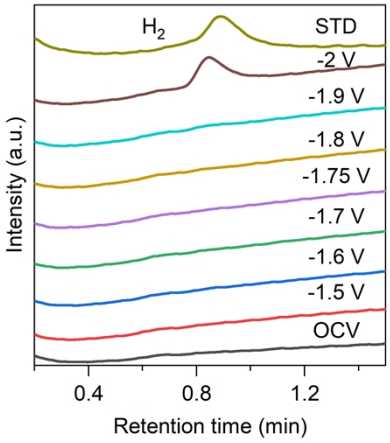


***Figure S7.*** Gas chromatography (GC) analysis of silicotungstic acid reduction products at varying potentials.

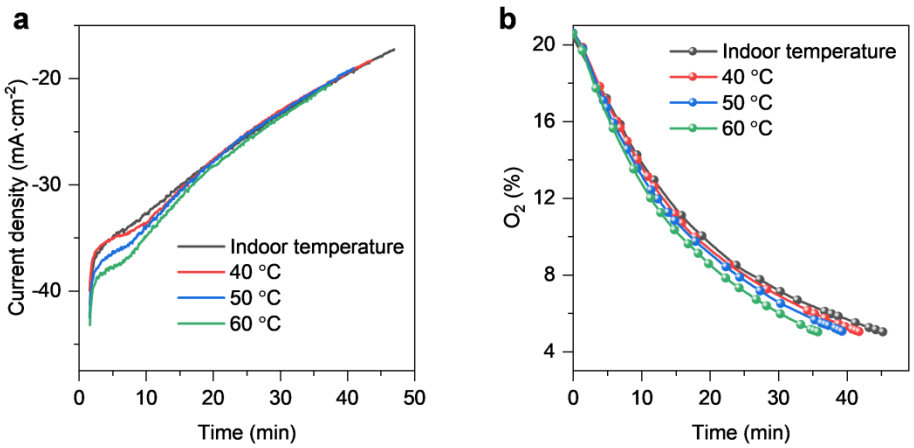


***Figure S8.*** (a) Deoxygenation rates and (b) corresponding current densities of silicotungstic acid solution at different temperatures.

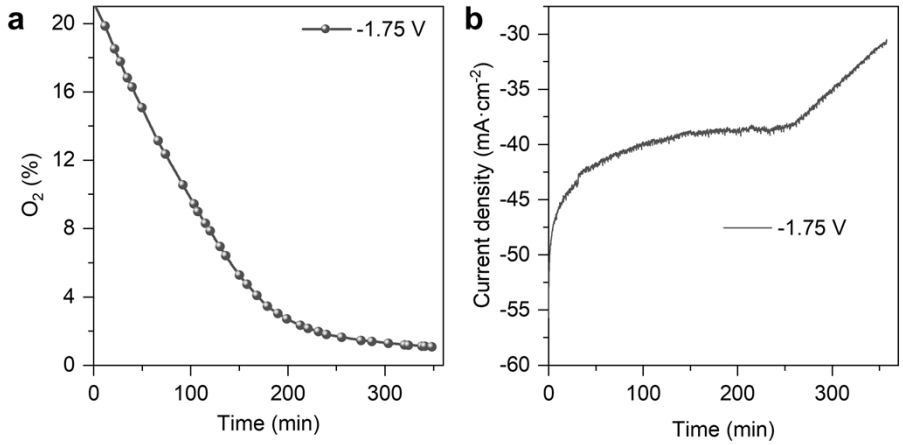


***Figure S9.*** Deoxygenation performance (a) and corresponding current profile (b) for a 500 mL container operated at -1.75 V.

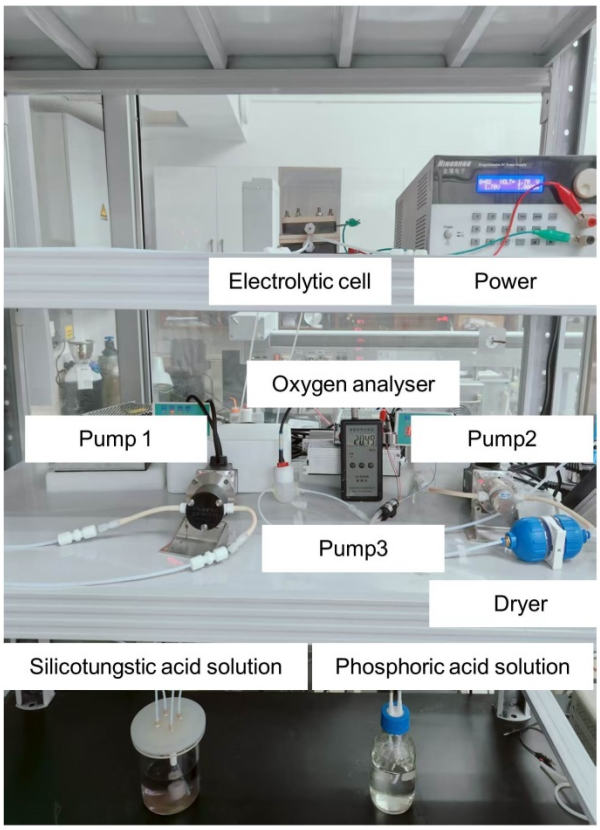


***Figure S10.*** Photograph of EMAORS under high circulation flow rate

*Note:*

1. Electrolytic cell (active area: 5 × 5 $cm^2$);
2. DC power supply;
3. Pump 1 (for circulating cathode electrolyte);
4. Oxygen analyzer;
5. Pump 2 (for circulating air);
6. Pump 3 (for circulating anode electrolyte);
7. Dryer (for removing entrained water vapor);
8. Silicotungstic acid solution;
9. Phosphoric acid solution.

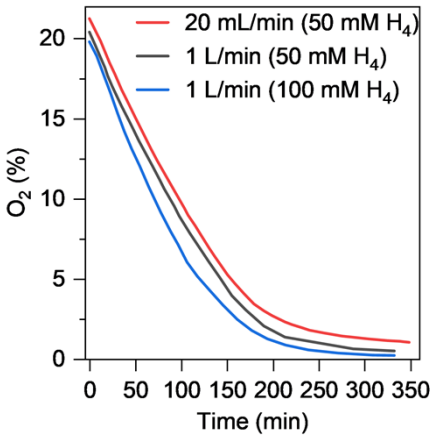


***Figure S11.*** Comparison of oxygen removal rates at different flow rates and various $H_4$ concentrations in a 500-mL closed system.

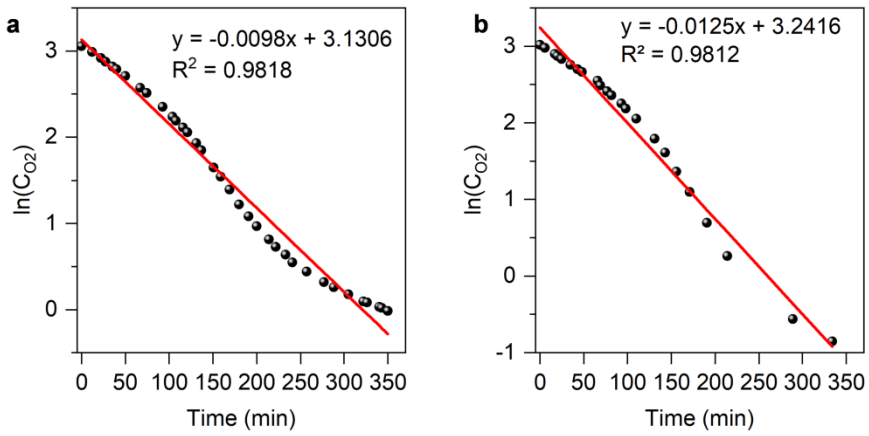


***Figure S12.*** Plot of ln ($C_{O2}$) versus time for 20 mL/min (a) and 1 L/min (b) flows.

Based on the electrochemical reaction mechanism between silicotungstic acid and oxygen, combined with the experimental data available, we have derived the kinetic mechanism for the deoxygenation of silicotungstic acid as a function of gas flow rate. The oxidation reaction of silicotungstic acid can be expressed as:

$$SiW_{12}O_{40}^{n-} + O_2 + H^+ \rightarrow SiW_{12}O_{40}^{m-} + H_2O$$

We fitted a quantitative relationship between the logarithm of oxygen concentration and deoxygenation time, demonstrating that the reaction follows first-order kinetics, i.e.,

$$r = k \cdot C_{O_2} \cdot C_{H_{5/6}}$$

$$k = Ae^{-\frac{E_a}{RT}}$$

Where r is the reaction rate, k is the rate constant, CO2 is the oxygen concentration, CH5/6 is the concentration of reduced H5 and H6, Ea is the activation energy, R is the gas constant, and T is the temperature. Since $H_5$ and $H_6$ are continuously generated at a constant potential during the reaction, we assume that the concentration CH5/6 remains constant. Therefore, the rate constants were determined as:

$$k' = k \cdot C_{H_{5/6}}$$

$k'_1$= 0.0098 $min^{-1}$ (at an air flow rate of 20 mL/min), $k'_2$ = 0.0125 $min^{-1}$ (at an air flow rate of 1 L/min). According to the mass transfer theory, the rate of oxygen consumption is related to the mass transfer coefficient ($k_L \cdot \alpha$) and the oxygen concentration $C_{O2}$ as:

$$k' = k_L \cdot \alpha \cdot C_{O_2}$$

The mass transfer coefficient is related to the pipe wall roughness, fluid viscosity, temperature, etc. Since all other conditions are the same, the following law can be obtained:

$$\frac{k'_2}{k'_1} = \left(\frac{Q_2}{Q_1}\right)^n = \left(\frac{1000}{20}\right)^n = \frac{0.0125}{0.0098} = 50^n$$

$n=0.0621$，$k' \propto Q_{gas}^{0.0621}$

Q denotes the gas flow rate. The kinetic analysis presented above indicates that the reaction rate between silicotungstic acid and oxygen is only weakly dependent on the gas flow rate. This conclusion is supported by the relatively small variation in the apparent rate constants ($k'_1$ and $k'_2$) under significantly different flow conditions (1 L/min vs. 20 mL/min).

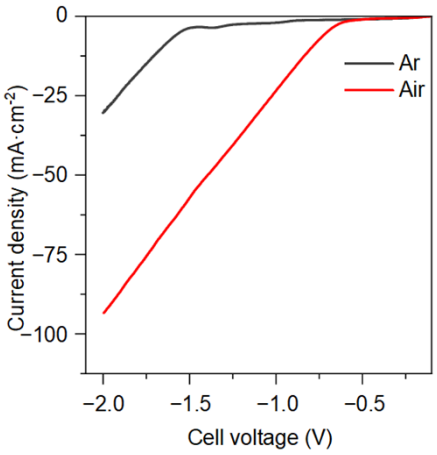


***Figure S13.*** LSVs of the ORR system with commercial Pt/C catalysts in Ar and in air.

*Note:* The performance comparison between the acidic EMAORS system and the alkaline Pt/C ORR system in this study is based on the premise that each system operates under its most common and optimized chemical environment. Although the reaction media pH differs, the primary objective of this comparison is to evaluate the overall efficiency, stability, and economic viability of two fundamentally distinct technological pathways for achieving the same application goal: efficient gas-phase deoxygenation. This approach highlights the unique advantages and innovative value of EMAORS in circumventing the reliance on precious metal catalysts and alkaline electrolytes inherent in conventional ORR technology.

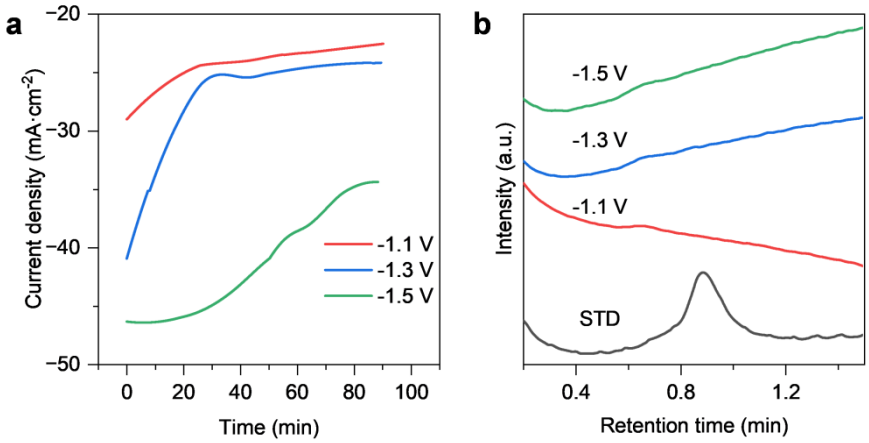


***Figure S14.*** (a) ORR current of Pt/C catalysts at -1.1 V, -1.3 V, and -1.5 V. (b) GC monitoring of hydrogen evolution during Pt/C operation at different potentials.

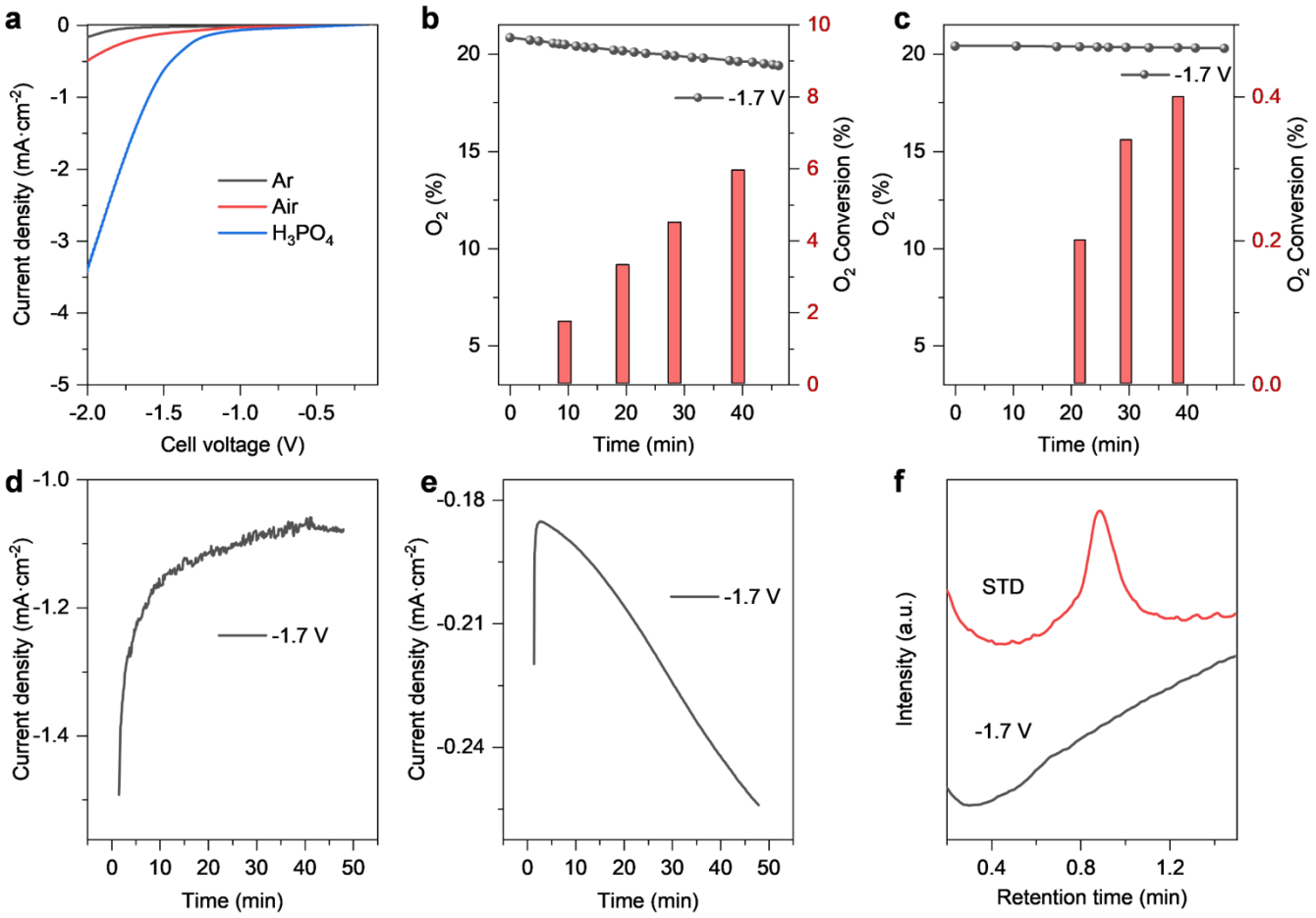


***Figure S15.*** (a) LSV curves of carbon felt under argon, air, and phosphoric acid-only electrolyte. (b) Deoxygenation rate and corresponding oxygen conversion rate when air is directly introduced into carbon felt. (c) Deoxygenation rate and corresponding oxygen conversion rate using phosphoric acid-only electrolyte. (d) Current curves with direct air flow into carbon felt. (e) Current curves using phosphoric acid-only electrolyte. (f) GC analysis of reduction products in phosphoric acid-only electrolyte.

*Note:* At -1.7 V, no hydrogen was detected via GC when using a phosphoric acid-only electrolyte.

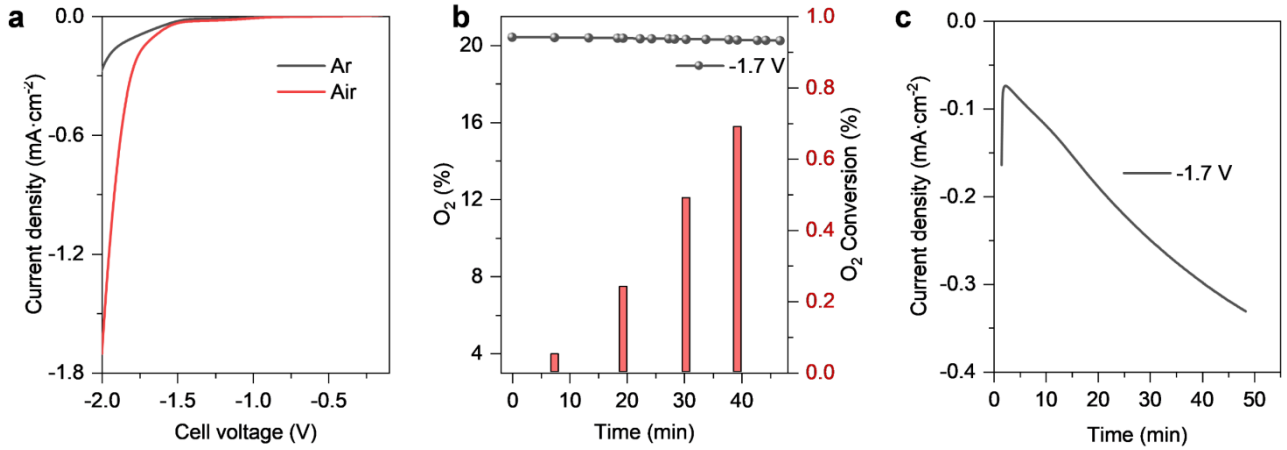


***Figure S16.*** Deoxygenation performance of carbon paper (GDL-3250) cathode: (a) LSV curves under argon and air flow. (b) Deoxygenation rate and corresponding oxygen conversion rate at -1.7 V. (c) Current curves at -1.7 V.

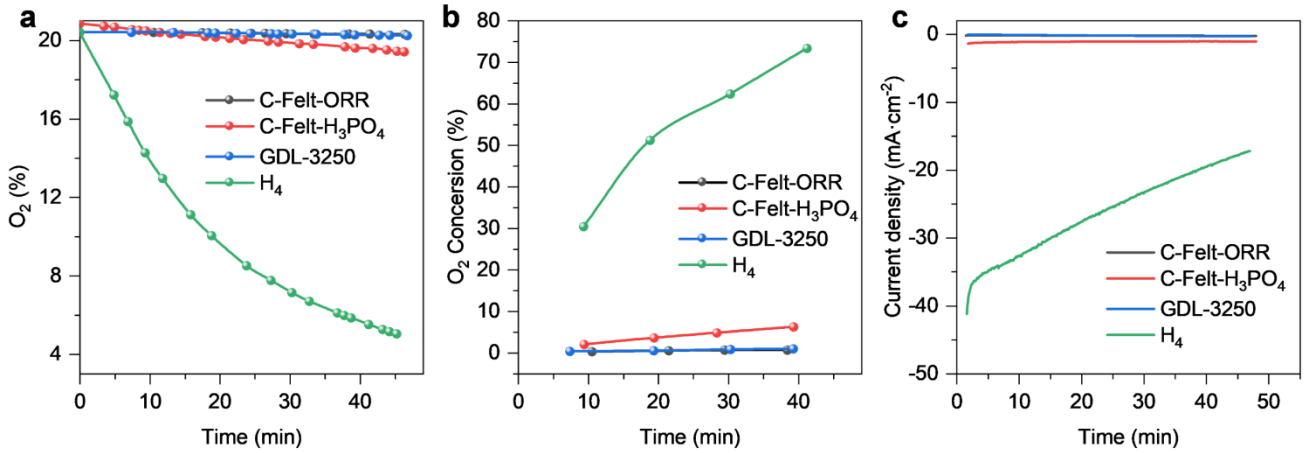


***Figure S17.*** Comparison of deoxygenation performance under different configurations (a), with the corresponding $O_2$ conversion rates (b) and current curves (c).

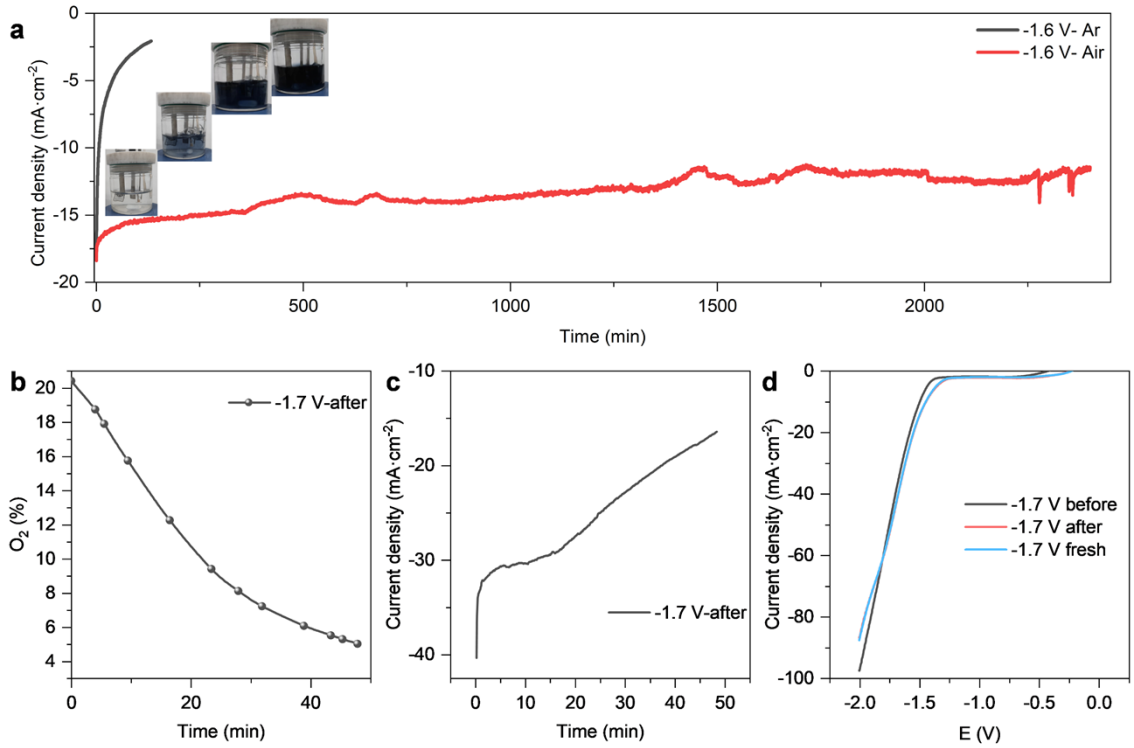


***Figure S18.*** Stability assessment of silicotungstic acid solution: (a) Current profiles under continuous argon and air flow. (b) Deoxygenation rate after the cycling reaction under constant oxygen flow. (c) Current profile at -1.7 V post-air exposure. (d) LSV curves of initial and post-reaction silicotungstic acid.

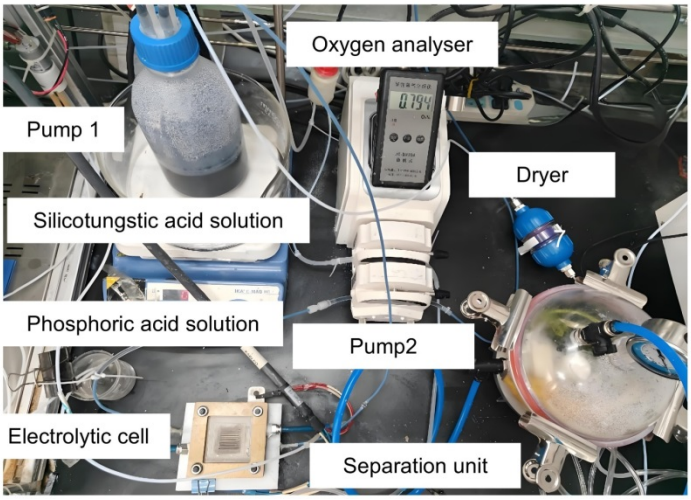


***Figure S19.*** Photograph of the EMAORS.

Note:

1. Pump 1 (for circulating anode electrolyte);
2. Silicotungstic acid solution;
3. Phosphoric acid solution;
4. Electrolytic cell (active area: 2 × 2 $cm^2$);
5. Oxygen analyzer;
6. Pump 2 (dual channels for circulating cathode electrolyte and air, respectively);
7. Dryer (for removing entrained water vapor);
8. Separation unit.

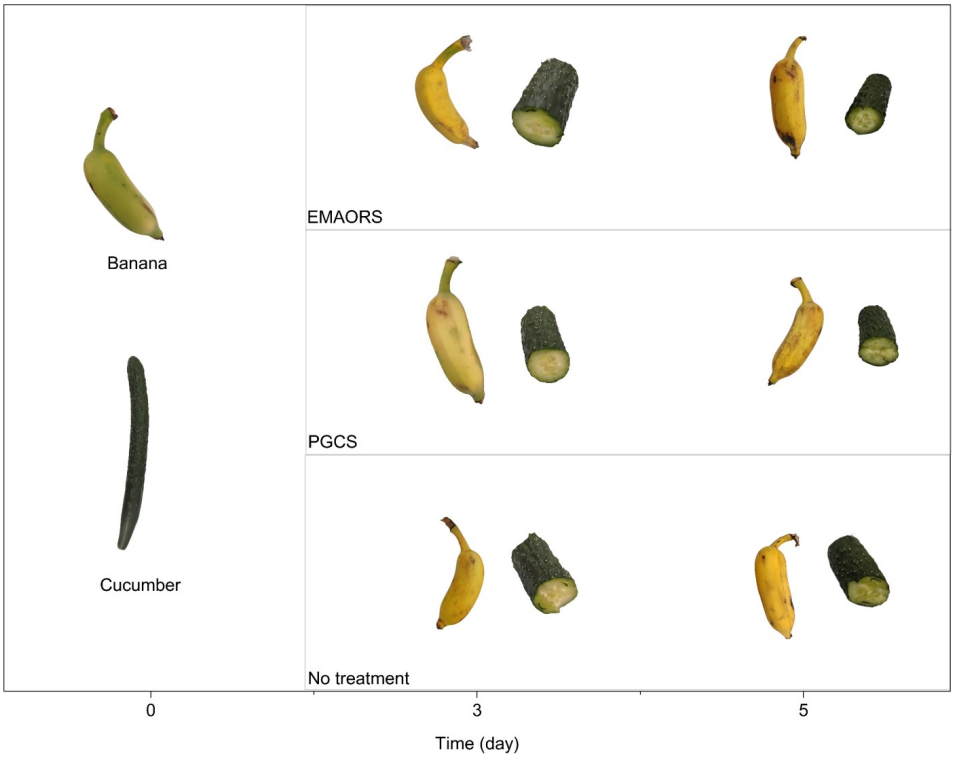


***Figure S20.*** Visual comparison of bananas and cucumbers stored in EMAORS, PGCS, and ambient conditions for 3 and 5 days.

Note: Cucumbers softened significantly in the PGCS and ambient groups due to ethylene synthesis being accelerated by oxygen[4]. Banana peels showed no visible differences.

***Table S1.*** Sensory evaluation of milk under different preservation methods.

| **Group** | **Odor** | **Organization** | **Color** | **pH (Fresh milk: 6.78）** |
|---|---|---|---|---|
| EMAORS | Strong milk aroma | Homogeneous, no precipitate | Milky white | 6.77 |
| PGCS | Rancid odour | Precipitate, slight whey separation | Slight yellowing | 6.65 |
| No-treatment | Strong rancid odor | Curdled lumps, heavy whey separation | Yellowish | 6.49 |

*Note:* Sensory evaluation is critical for assessing dairy quality, including flavor and aroma.[5]

***Table S2.*** Cost analysis of the EMAORS

| **Species** | | **Cost (USD)** |
|---|---|---|
| **Electrode assembly** | Cathode | 4.18 |
| | Anode | 20.9 |
| | Cation exchange membrane | 2.234 |
| | **Individual total** | **27.314** |
| **Device fittings** | Electrolytic cell (two unipolar plates) | 164.392 |
| | End plate | 20.548 |
| | Other components | 6.164 |
| | **Individual total** | **218.418** |
| **Gas-liquid Circulation system** | Air pump, liquid pump and liquid storage device | 31.507 |
| | Gas-liquid separator | 11.644 |
| | **Individual total** | **43.151** |
| **Total** | | **288.883** |

***Table S3.*** Multiparameter analysis of the EMAORS，ORR and GAPS Reactor.

| | **EMAORS** | **ORR[6]** | **GAPS Reactor[7]** |
|---|---|---|---|
| **$O_2$ removal rate ($mL \cdot min^{-1}$)** | 0.35 | 36.33 | 14.06 |
| **Equipment cost (USD)** | 288.883 | 433.1 | 7.411 |
| **Energy consumption ($kWh \cdot L^{-1}$ $O_2$)** | 0.013 | 0.016 | 0.014 |
| **Maintenance frequency** | 0 | Once a year | 0 |
| **Total cost of ownership (USD)** | 288.883 | 1436.4 | 7.411 |
| **Area-normalized $O_2$ removal rate ($mL \cdot min^{-1} \cdot cm^{-2}$)** | 0.09 | 0.15 | 0.14 |
| **Minimum residual oxygen concentration (%)** | 0.4 | 0.7 | 10 |

*Note*：The specific energy consumption reported refers to that required for reducing $O_2$ to <1% in a 500 mL chamber at -1.7 V. To ensure the fairness and consistency of the energy consumption comparison, the specific energy-consumption values reported in this study refer exclusively to the electrical energy consumed by the electrolyzer during deoxygenation. This calculation scope deliberately excludes the energy consumption of auxiliary equipment, such as gas/liquid circulation pumps. This approach is adopted primarily because the type, power, and operational efficiency of auxiliary components can vary significantly across different system configurations. Their inclusion would introduce additional variables and obscure the objective assessment of the core electrochemical deoxygenation efficiency.

## References


1 Q. Wu, S. Ji, J. Chen, X. Tan, W. Ong, R. Du, P. Wang, H. Wang, Y. Qiu, K. Yan, Y. Zhao, W. Zhao, K. Peng, Y. Chen, S. Hung, L. Zhou, X. Wang, G. Qiu and G. Chen, *Nature Water*, **2025**, 1-12.

2 P. Wang, A. Pei, Z. Chen, P. Sun, C. Hu, X. Wang, N. Zheng and G. Chen, *Nat. Commun.*, 2025, **16**, 731.

3 N. Elgrishi, K. J. Rountree, B. D. McCarthy, E. S. Rountree, T. T. Eisenhart and J. L. Dempsey, *J. Chem. Educ.*, 2018, **95**, 197.

4 B. M. Hurr, D. J. Huber, C. E. Vallejos and S. T. Talcott, *Postharvest Biol. Technol.*, 2009, **52**, 207.

5 A. N. Schiano, W. S. Harwood and M. A. Drake, *J. Dairy Sci.*, 2017, **100**, 9966.

6 Y. Tan, R. Ma, M. Jiang, J. Mao, D. Li, C. Zhao, F. Zhou, P. Li, Y. Zhang, Z. Jiang, S. Lin, Z. Wang, Y. Zhang and Y. Wu, *Device*, 2025, **3**, 100710.

7 P. Li, X. Tang, X. Zhou, C. Zhao, W. Shen, Y. Tan, D. Li, P. Jiang, F. Zhou, Z. Wang, J. Tang, G. Li, Y. Zhang and Y. Wu, *Nat. Commun.*, 2025, **16**, 4309.